



Enabling the dynamic simulation of an unaggregated, meshed district heating network with several thousand substations

Jan Westphal ^{a,*}, Johannes Brunnemann ^b, Arne Speerforck ^a

^a Institute of Engineering Thermodynamics, Hamburg University of Technology, Denickestr. 17, Hamburg, 21073, Germany

^b XRG Simulation GmbH, Harburger Schlosstraße 6-12, Hamburg, 21079, Germany

ARTICLE INFO

Keywords:

District heating network
Large-scale
Dynamic simulation
Modelica

ABSTRACT

District heating networks (DHN) are an essential part of the decarbonization of the heating sector. As a high proportion of the buildings provided with district heating are integrated into larger networks, there is a need for efficient simulation tools that enable the simulation of large-scale DHN. This paper introduces a modeling concept for the dynamic simulation of DHN with several thousand substations using the modeling language Modelica. The emphasis is on the simulation of strongly meshed networks, usually appearing in large-scale DHN. To test the modeling concept, a generic, large-scale DHN is designed and simulated. The results are used to determine the time constants of the DHN for different load cases and evaluate the efficiency of the heat provision. We show that our modeling concept is suitable to simulate a DHN with 2167 substations, while the results suggest that there is still room for upscaling. To make the modeling concept fully open-source, a smaller DHN model is designed and simulated in OpenModelica. A comparison to Dymola shows that Dymola is not only 15 times faster in terms of simulation time; it also needs much less time for the translation and compilation of the model, highlighting future development of OpenModelica.

1. Introduction

1.1. Motivation

In recent years, the efficiency of district heating networks (DHN) as well as the optimal use of primary energy sources have become increasingly important. In particular, the possibility of integrating waste heat and renewable energies is a valuable advantage of DHN. DHN are classified into four generations described in [1]. In Europe and Germany, third-generation DHN are widely spread. A high share of the heat supply distributed by DHN is provided by large-scale DHN. For example, cities like Hamburg, Berlin, or Dresden own DHN with several thousand substations.

Due to the challenges that occur within the necessary transformation and expansion planning, suitable tools are needed for the simulation of large-scale DHN [2]. For instance, the optimization of the temperature control used by many DHN is a possible use case for dynamic simulation [3]. Adapting the supply temperature with consideration of the thermal inertia of the network can be used for load shifting and, therefore, can decrease peak heat production. Another use case is the storage of surplus electricity in DHN for the better integration of fluctuating renewable energies [3]. However, also planning for grid expansion combined with the integration of fluctuating

heat sources raises the challenge of ensuring the security of supply for every consumer. To investigate these use cases and bring them into application, it is crucial that simulation tools can efficiently simulate larger-scale DHN.

This paper introduces a fully open source modeling concept for the dynamic simulation of large-scale district heating networks with the objective of bringing the simulation tool into application. In further research, this modeling concept shall be used for supply temperature optimizations and the reduction of peak production due to load shifting.

In the first section, the scope of the paper is explained. The second section focuses on the latest modeling concepts and delineates them from our modeling approach. In the third section, we introduce our modeling concept and its methodology. To prove the applicability of the concept, we present simulation results for a DHN with more than two thousand substations. Finally, our findings are summarized and we outline directions for our future work.

1.2. Research gap

One of the main issues concerning the dynamic simulation of district heating is the simulation of large-scale DHN [4–6]. To the authors best knowledge, there is no publication featuring a dynamic simulation of

* Corresponding author.

E-mail address: j.westphal@tuhh.de (J. Westphal).

a DHN with more than a thousand consumers, as models that allow consideration of thermal inertia are normally limited to a few hundred substations. However, such simulations are necessary to investigate the described use cases for the DHN of larger cities like Berlin or Hamburg. Moreover, in [6] it is stated that there are limited papers on mathematical optimization, and existing studies on DHN simulations mainly focus on specific case studies. This paper tries to close this gap by analyzing the solution process of a DHN model in Modelica [7] and suggests options to avoid the specific problems of DHN simulations like the appearance of non-linear equations, a huge number of states, or unnecessary iterations. A numerically performant modeling approach for the dynamic simulation of large-scale DHN is presented and its applicability is shown by a DHN simulation with 2167 substations.

An issue with using Modelica is that mostly the software Dymola [8] is used to simulate larger models [9,10]. Although Modelica is a free open source modeling language, Dymola is a commercial, chargeable simulation tool. As a result, simulations done with Dymola cannot be seen to be fully open source. However, with OpenModelica [11], there is a fully open source software environment. For this reason, the modeling concept introduced in this paper is created to enable large-scale simulations not only in Dymola but also in OpenModelica.

2. Pipe network simulation - literature review

2.1. Modeling of district heating networks

In the literature, the modeling concepts for DHN are normally classified by their calculation method and the investigated system behavior [6,12]. The calculation method refers to the process of solving the hydraulic and thermal problems. It is differentiated between methods that solve the hydraulic problem separately from the thermal problem and methods that use an integrated approach [6]. The behavior of the system is categorized into dynamic and steady-state methods [12]. Inside this category a division between models that are fully dynamic and, therefore, are considering hydraulic as well as thermal dynamics and models that only consider thermal dynamics can be done. Moreover, it is differentiated between the control strategies of the DHN. There are three common control strategies: Constant temperature and variable flow control (CT-VF), variable temperature and constant flow control (VT-CF) and variable temperature and variable flow control (VT-VF) [6]. Some simulation tools are designed to represent one specific control strategy [6].

In Modelica there are open source libraries that can be used for the dynamic simulation of DHN. Modelica is a modeling language that in recent years became popular in research topics of DHN simulations due to its equation-based and object-oriented character [6]. Furthermore, Modelica enables dynamic simulation and bidirectional flow. Libraries that can be used for the simulation of DHN in Modelica are, for example, the ClaRa [13], the TransiEnt [14], and the IBPSA library [15].

The ClaRa library is based on balance equations for mass, energy, and momentum which are discretized using a finite volume approach on a staggered grid. The use of the TIL media library [16] enables the investigation of two-phase flows. Therefore, the models are very detailed and designed for the investigation of specific effects in power plants and other components. The TransiEnt library is a library for the dynamic simulation of integrated energy grids. It is based on the ClaRa library and therefore uses a similar modeling concept for the pipe and junction models. However, it has a wide variety of models and also features a plug-flow model, which was used and further explained in [17].

Using a plug-flow or Lagrangian approach for considering the thermal dynamics became popular in recent years and has been used in various publications since then e.g. [17–20]. In the IBPSA library, a pipe model based on the plug-flow approach was created [18]. It uses the in Modelica implemented spatialDistribution operator [7] to

track single fluid particles along a stream and, therefore, can take time delays into account. Because this approach enables the consideration of thermal inertia without the use of a huge number of states, it is considered an efficient approach. The temperature losses along the pipe are calculated with an analytical solution of the energy balance, and the inertia of the pipe wall is considered with a model of lumped heat capacity. The pipe model of the IBPSA library was validated with measured data and is known to have good accuracy [4,18]. Based on the IBPSA library, the DisHeatLib library was created, which provides component models for the simulation of DHN, like pump models and detailed models of substations [21].

In [22] a robust modeling concept for the efficient creation and simulation of thermofluidstream models like cooling systems for airplanes or cars is presented. The modeling concept takes advantage of the fact that computational fluid dynamics (CFD) normally has a high number of states, which can cause a huge computational effort. Algebraic modeling, on the other hand, can lead to large non-linear systems with unknown solvability. The presented solution in [22] uses mass flow states to avoid implicit non-linear systems and trades them against implicit linear systems, which are much easier to solve.

The Python package PandaPipes [23] is a table-based tool for the static simulation of DHN in Python. It uses a separate calculation of the hydraulic and thermal parts of the network. The algebraic equations are solved with a Newton solver and the handling of the simulations is numerically robust and user-friendly. According to the authors experience, PandaPipes is a good tool for the static simulation of larger district heating networks. A commercial tool that is sometimes used in research is Stanet [24] which, for example, was used in [23,25].

In [26] the authors developed a modeling approach to simulate DHN of arbitrary size. A coupled calculation of the hydraulic and the thermal part is done and the thermal dynamics of the network are considered using an improved plug-flow approach. The modeling concept is tested and compared to a model created with the Modelica standard library for a smaller DHN simulation [26].

The modeling approach developed in this paper is a coupled approach that solves the hydraulic and thermal problem together. It is based on the three balance equations but only considers the dynamics of the thermal problem. The energy balance is discretized with a finite-volume approach, and therefore no plug-flow approach is used. Various control strategies can be investigated, but it is designed to represent a DHN with a temperature and flow control.

2.2. Simulation of large-scale DHN

So far, the simulation of large-scale DHN is often done via the use of aggregation methods e.g. [27–29]. However, these aggregation methods are producing an error due to the simplifications made. This is especially the case, as those aggregation methods refer to a certain load state, and therefore the error produced in all-year simulations is often difficult to assess. Moreover, for the practical application of simulation tools, an aggregation may not be suitable as key locations in the grid might not be represented [20] and the security of supply cannot be guaranteed for every consumer.

Another approach for the simulation of large-scale DHN is to neglect dynamic effects and perform a steady-state simulation e.g. [23,30]. Nonetheless, this concept does not allow the consideration of thermal inertia like the piping network or thermal storage. As a result, optimizations of central or decentralized heat storages as well as using the thermal inertia of buildings cannot be investigated with such tools. Furthermore, this method is less accurate as the effect of the propagation of a supply temperature change on the heat losses cannot be considered.

Several publications deal with the dynamic simulation of DHN, but as already mentioned, none of them deal with simulations of DHN with more than several hundred substations. For example, in [31], a DHN with 250 consumers is autogenerated based on open street map. It is simulated dynamically with models of the IBPSA library [15]. In [25],

the creation of a network topology is validated with a real DHN. For this purpose, the simulation tool Stanet [24] was used to simulate a DHN with 200 substations. [32] features a simulation of the DHN of Turin, which is a large district heating system. However, in this simulation, only the 70-km transport network with 182 distribution networks was considered. A similar network was also used for a static simulation to determine the optimal location of a large heat pump in a DHN [30]. [5] used the pipe model of [33] to create a simulation of a district heating and cooling network in Dymola with over 100 consumers and optimize it. In the publication of [33], the author states that 100 consumer models is the largest number of consumers the modeling concept can handle at the moment. Nonetheless, the publication is from 2016, and it is noted that there is room for improvements to be made. Another small DHN was simulated in [34] to determine the time constants of the grid and the buildings with the objective of using this thermal inertia for peak shaving.

One of the largest dynamic simulations found in the literature is the work of [35], where a network with 413 substations is validated using measurements from a real network. In [36], the design of a 160-consumer DHN is considered large-scale. This also holds true for the work of [10] where a discretized, dynamic model of a DHN is solved using the solver Cvode. Here, a 5th-generation DHN with 180 distributed heat pumps is simulated with good results regarding efficiency and computational effort. The DHN of the city of Rostock was simulated in [37] using the models of the ClaRa library [13,38]. However, for this simulation, the network was widely simplified.

The review of the publications concerning the simulation of large-scale DHN shows that most simulations are limited to a few hundred consumers, or at least until now, it has not been proven otherwise. This leaves room for improvement, as most of the DHN considered large-scale are only a few kilometers long with a few hundred consumers, but DHN in larger cities like Berlin, Hamburg, or Dresden can easily reach several hundred kilometers and tens of thousands of substations.

3. Modeling concept

In this paper, the modeling language Modelica is used. Modelica is an acausal and object-oriented modeling language that is suited for performing dynamic simulations. The equation-based character and the automatic processing of time derivatives enable the description of physical behavior with algebraic and ordinary differential equations. For developing a model that is capable of running an efficient dynamic simulation, it is key to design the component models as numerically robust as possible. Therefore, the component models have to suit the issue, and simplifications have to be made. There are three key points that ensure an efficient design of the DHN model created in this paper. These are:

1. Use of a suitable consumer model and mass flow states to avoid non-linear implicit systems in the algebraic part of the system of equations inspired by [22]
2. Avoidance of unnecessary equations, for example, assumption of constant fluid properties like density, specific heat capacity or dynamic viscosity
3. Enabling a robust simulation due to discretization of only the energy balance to utilize sparse properties of the occurring matrices

For example, the avoidance of dynamic media models simplified the handling of the simulations by a lot and improved the applicability. This approach seems justified as the only medium used in DHN is water and no relevant chemical reactions occur.

In general, five main components are needed for the simulation of a district heating grid. These are: a pipe model, a consumer model, a junction model, a producer model, and a pump model. The three balance equations for energy, mass, and momentum form the basis for all of these components. All of them use the Modelica stream connector described in [39], enabling flow reversal in every component. In the following section, these component models will be described.

3.1. Pipe model

The pipe model uses a static mass balance described in Eq. (1). The definitions of the different variables from the following equations can be found in the table of abbreviations at the end of the paper.

$$\dot{m}_{in} + \dot{m}_{out} = 0 \quad (1)$$

There is no consideration of mass storage effects or density changes. This is an often-made assumption for the simulation of DHN [9]. As a result, no pressure states are used in this model. A dynamic momentum balance is used to describe the pressure loss over the pipe. However, it is not used in every pipe, as will be explained later in Section 3.7. The starting point for deriving the momentum balance is Eq. (2), which was derived in [22].

$$\frac{d\dot{m}}{dt} \cdot \int_{s_1}^{s_2} \frac{1}{A} ds + \Delta q = \Delta p - \Delta p_{ext} \quad (2)$$

The acceleration of a particle in the fluid due to a shift of the particle in the flow field is neglected, so Δq becomes zero. The pressure loss due to external forces Δp_{ext} consists of the friction pressure loss. To calculate the pressure loss due to friction, a pressure loss model of a straight pipe from the fluid dissipation library described in [40] was used. It uses the Darcy–Weisbach equation for determining the pressure loss and considers different flow regimes. In [22], the remaining integral term is defined as the inertance L (3).

$$L = \int_{s_1}^{s_2} \frac{1}{A} ds \quad (3)$$

Using the inertance L and the fluid dissipation pressure loss model results in (4).

$$\Delta p = \frac{d\dot{m}}{dt} \cdot L + \lambda \cdot \frac{l}{d} \cdot \frac{\rho}{2} \cdot \left(\frac{\dot{m}}{\rho \cdot \frac{\pi \cdot d^2}{4}} \right)^2 \quad (4)$$

λ is the pipe friction coefficient, l is the length of the pipe, d is the diameter of the pipe and ρ is the density of the fluid. The benefits of the introduced mass flow states are further discussed in Section 3.7. Other external forces than friction, like gravity, have been neglected, although they could easily be included if they were of interest. The thermal behavior of the pipe is described by a dynamic energy balance for an open system, which can be seen in Eq. (5).

$$\rho_f \cdot (V_f + V_w) \cdot \frac{du_n}{dt} = \dot{m}_{in} \cdot h_{in} + \dot{m}_{out} \cdot h_{out} + \dot{Q}_{loss} \quad (5)$$

To set up this equation, a thermal equilibrium between the fluid and the pipe wall was assumed. The volume of the pipe wall has been converted to an equivalent water volume V_w . This made it possible to regard the thermal inertia of the pipe wall, which is necessary according to [41]. To add the thermal capacity of the pipe wall to the capacity of the water is described in [41] as the most efficient way of taking the wall inertia into account. It can be seen that potential and kinetic energy have been neglected. Only mass transfer in the flow direction and heat transfer perpendicular to the flow direction have been considered. The energy balance was discretized with the upwind discretization scheme, which uses a case distinction depending on the flow direction (see Fig. 1).

This method enables efficient discretization without using too many variables. Further information about this type of discretization can, for example, be found in [10]. Because the mass balance is stationary, and the fluid properties are constant, there is no need to discretize all of the balance equations but only the energy balance. This reduces the number of states and variables and leads to a sparse Jacobi-matrix of the generated system of ordinary differential equations.

Using the plug flow concept was also considered for the pipe model. However we found, that usage of the spatial distribution operator can lead to numerous rejected solver time steps. Therefore, it can make a simulation inefficient, as will be explained further in Section 3.6. This

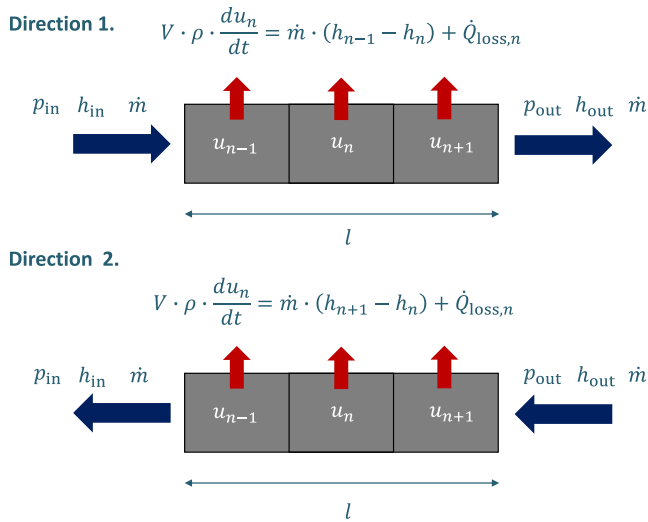


Fig. 1. Discretized pipe with different flow directions.

is especially the case for larger networks containing many pipes with different time constants. Moreover, the heat losses for a state change can be accessed more accurately with a discretized pipe model, as the computation of the heat losses in the plug flow pipe are not valid for sudden temperature changes and flow reversal. Finally, the use of a high number of spatial distribution operators lead to problems when testing DHN simulations in OpenModelica. Heat losses are considered with a constant heat loss factor of $U = 0.3 \text{ W m}^{-1} \text{ K}^{-1}$. This heat loss factor U is normally part of the data sheets of the pipes. The heat losses are calculated with Eq. (6).

$$\dot{Q}_{\text{loss}} = U \cdot \Delta x \cdot (T - T_{\text{ground}}) \quad (6)$$

where \dot{Q}_{loss} is the heat loss to ground, U is the heat loss factor, Δx is the discretized length of the pipe, T is the temperature of the pipe and T_{ground} is the temperature of the surrounding ground.

3.2. Junction

The junction model used in this publication is a model to split or join mass flow rates. It contains a lumped control volume with a dynamic energy balance and a stationary mass balance. There is no consideration of heat losses, and for pressure loss, a linear pressure loss model is assumed.

3.3. Heat pump

The heat pump model is a stationary model of a heat pump. It is used to calculate the needed electric power from a given heat flow rate. The Carnot COP of the heat pump is calculated with the supply temperature, the temperature of the heat source, and an internal temperature difference with Eq. (7) similar to [42]

$$COP_{\text{Carnot}} = \frac{T_{\text{supply}} + \Delta T_{\text{internal}}}{(T_{\text{supply}} + 2 \cdot \Delta T_{\text{internal}}) - T_{\text{source}}} \quad (7)$$

$\Delta T_{\text{internal}}$ is 5 K and T_{source} is assumed to be 20 °C. A constant efficiency factor $\eta_{\text{hp}} = 0.45$ is assumed to calculate the COP from the Carnot-COP, which is described in Eq. (8)

$$COP = \eta \cdot COP_{\text{Carnot}} \quad (8)$$

With the COP and the given heat flow rate, the needed electric power can be determined with Eq. (9)

$$P_{\text{el}} = \frac{\dot{Q}}{COP} \quad (9)$$

The specific enthalpy at the outlet of the heat pump is calculated with the needed heat flow rate, the inlet temperature of the heat pump, and the mass flow rate provided by the pump described in Eq. (10).

$$h_{\text{out}} = h_{\text{in}} + \frac{\dot{Q}}{\dot{m}} \quad (10)$$

3.4. Pump

The pump model is a stationary model for the calculation of the needed electric pumping power. It provides a pressure difference and calculates the needed electric power for a given mass flow rate, a provided pressure difference and an efficiency factor (11).

$$P_{\text{el,pump}} = \frac{\dot{m} \cdot \Delta p}{\eta_{\text{el}}} \quad (11)$$

An efficiency factor of $\eta_{\text{el}} = 0,9$ is assumed.

3.5. Consumer

The consumer model has two purposes. Firstly, it calculates the heat flow rates needed for the household at a given ambient temperature. Secondly, it determines the required mass flow rate from the calculated heat flow rate. It contains five subcomponents: a heat capacitor, a thermal conductance, a P-controller, a pump, and a heat exchanger. The structure of the model can be seen in Fig. 2.

The heat capacitor represents the thermal inertia of the buildings with an average room temperature, described in (13). With this temperature, the heat conductance, and a given ambient temperature, the heat flow rate loss from the building is calculated with Eq. (12).

$$\dot{Q}_{\text{house}} = G \cdot (T_{\text{room}} - T_{\text{amb}}) \quad (12)$$

$$C \cdot \frac{dT_{\text{room}}}{dt} = \sum \dot{Q} \quad (13)$$

The parameters C and G have been calibrated with a detailed building model built in [43]. It represents a single-family household with the German KFW 55 insulation standard. However different house types can be considered for each consumer if needed.

The heat exchanger transfers the heat from the fluid to the building using a lumped energy balance described in Eq. (14) and a linear heat transfer model described in Eq. (15). The factor kA is the product of the heat conductance and the area of the heat exchanger.

$$V_{\text{hex}} \cdot \rho_f \cdot \frac{du_{\text{hex}}}{dt} = \dot{m} \cdot (h_{\text{in}} - h_{\text{out}}) + \dot{Q}_{\text{hex}} \quad (14)$$

$$\dot{Q}_{\text{hex}} = kA \cdot (T_f - T_{\text{room}}) \quad (15)$$

It is designed for the maximal transferred heat flow rate and a temperature difference of 30 K.

The mass flow rate is controlled by the P-controller, which gets a set value for the room temperature and regulates the mass flow rate through the pump to keep this temperature constant. The parameter of the P-Controller was set to $P = 10$. The steady state error which occurs due to the missing integrator part in the controller amounts to a maximum of 0.08 K and is therefore neglected. Normally, a consumer model would consist of a valve instead of a pump e.g. [5]. The opening of the valve would be regulated by a controller to set a mass flow rate with a given pressure difference. This, however, would create a dependency on the mass flow rate from the hydraulics of the overall system. In the chosen configuration, where the mass flow rate is being set directly by the controller, it only depends on the supply temperature and the needed heat flow rate. A deviation between those two cases would only occur if the pressure difference at the consumer would not be enough to enable the needed mass flow. This would not be the case for the regular operation. On the other hand, the decoupling of the mass flow from the pressure difference at the consumer avoids implicit non-linear systems of equations and leads to a massive reduction of the complexity of the system.

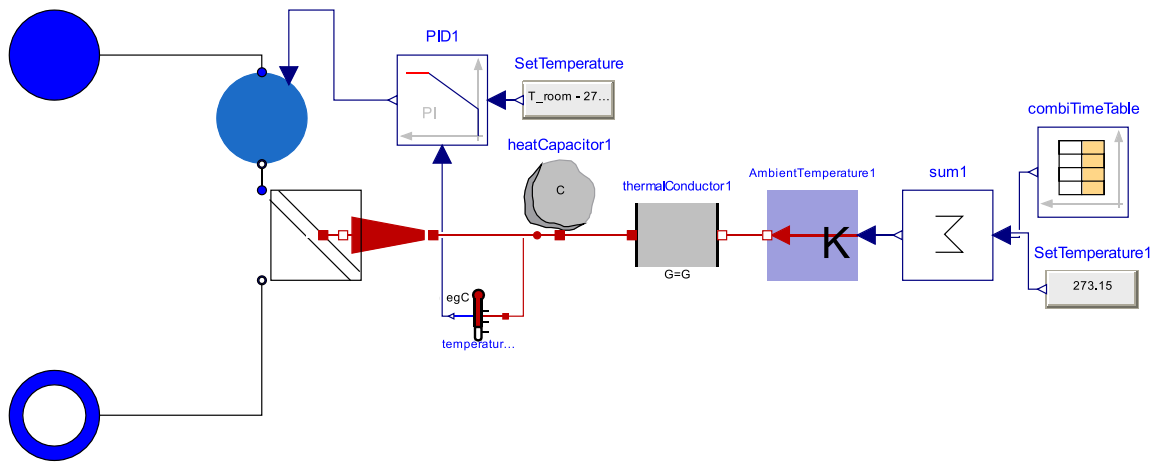


Fig. 2. Structure of the consumer model.

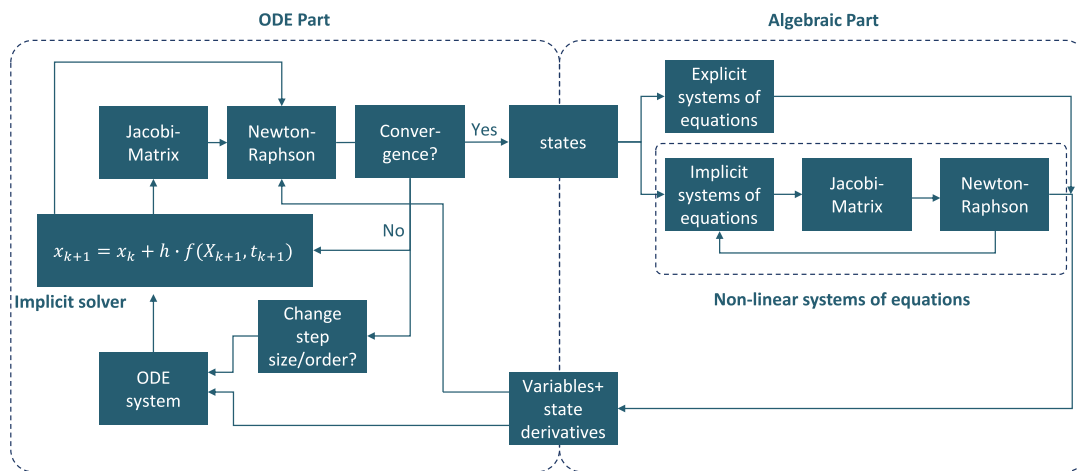


Fig. 3. Structure of the solution process.

3.6. Solution process of a modelica model

The general solution process of the Modelica model using a variable order and variable time step size solver such as DASSL [44] is shown in Fig. 3. It consists of an algebraic part and an ordinary differential equation (ODE) part. The states are part of the solution of the ODE part and are used to solve the algebraic part. The derivatives of the states are treated as unknowns in the algebraic part and are therefore a solution of the algebraic part. The calculated variables and state derivatives are transferred to the ODE part and used for the solution of the ODE part. If the algebraic part of the model is explicit, the system of equations can be solved easily by bringing the system matrix into block lower triangle form. The unknowns can then be calculated one by one without the use of iteration methods. However, if there are systems of equations that are implicit, they need to be solved iteratively. If these systems are also non-linear, a Newton–Raphson method is applied, which requires a lot of computational effort. This effort is especially high because the implicit system has to be evaluated for every time step of the ODE solver, which can be seen in Fig. 3.

The ODE system is solved with an implicit solver. For this paper, the Runge–Kutta based solver sdirk34hw available in Dymola is used. The resulting set of equations is therefore implicit and non-linear, so the Newton–Raphson method has to be applied. The more states a DHN model contains, the larger the Jacobian-Matrix gets. For solving this Newton-method, the variables and the state derivatives are needed for every iteration step. This means that the algebraic part of the model is solved for every step of the Newton iteration. After a Newton iteration

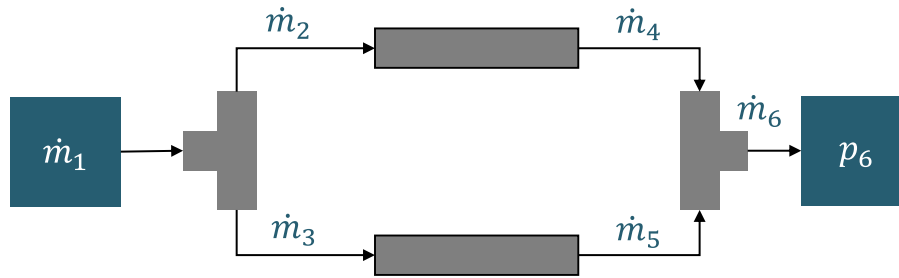
has done a maximum number of steps, the solver evaluates the accuracy of the step and checks for convergence. If the convergence criteria are not met, it rejects that step and tries again with a different step size or a different integrator order.

It can be concluded that especially rejected steps of the solver and large non-linear systems occurring in the algebraic part should be avoided to enable an efficient simulation of the model.

3.7. Handling of meshes

Implicit non-linear systems occur naturally in hydraulic simulations due to the non-linear character of the pressure loss and the meshing of the network. These non-linear systems can get especially large in DHN models because of the high number of nodes and meshes. However, we can avoid these non-linear systems with a strategic use of momentum states. The reason for this is that states are a solution of the ODE part and are therefore treated as known in the algebraic part. The right definition of states can consequently manipulate the algebraic system of equations in a way it becomes explicit. This leads to a shift of the computational effort from the algebraic part to the ODE part.

This method is very efficient if the ODE-part is a stable system and does not limit the step size of the solver. The idea behind this approach can be best understood with an example. In Fig. 4, a graphic of a hydraulic circuit of two parallel pipes is shown. The pipes are connected with a split and a join. The split and the join are connected with two boundary conditions. The split is connected to a mass flow source with a known mass flow rate and an unknown pressure. The



Screenshot of the statistics in Dymola:

```

Sizes of linear systems of equations: { }
Sizes after manipulation of the linear systems: { }
Sizes of nonlinear systems of equations: {7}
Sizes after manipulation of the nonlinear systems: {1}
Number of numerical Jacobians: 0
    
```

Fig. 4. An example of a hydraulic circuit.

join is connected to a sink with a known pressure and an unknown mass flow rate. Although this looks like a simple computation, this system of equations cannot be solved explicitly. The reason for this is that the mass flow rate going to each of the pipes is unknown and has to be calculated from the pressure difference. The pressure difference between the two pipes is also unknown and dependent on the mass flow rate. This system of equations can be solved easily if one mass flow rate through the pipes is known. This can be achieved with a mass flow state, as shown in Fig. 5. The mass flow derivative is an unknown in the algebraic part. On the other hand, the mass flow rate becomes known in the algebraic part, which is the point of this operation. The system of equations becomes fully explicit, as can be seen in Figs. 5 and 6. In Fig. 6 the sequence of the calculation of the variables is shown. Firstly, the mass flow rates can be calculated from the mass balances. This is not possible in the other scenario, as the splitting of the mass flow rate depends on the unknown pressures. After that, the pressures can be calculated with the given mass flow rates. Finally, the mass flow derivative is calculated. In Fig. 5, the Dymola screenshot of the translation shows that no implicit systems of equations occur in this set-up.

4. Verification

For the creation of the large-scale DHN model, different assumptions have been made to simplify the component models and ensure a robust and efficient simulation of the overall network. Therefore, there is a need for verification and validation to determine if the models can accurately describe the thermal behavior of DHN components. The focus of the verification is on the pipe model, which represents constant fluid properties. Moreover, it is the most important component model of the simulation, as it is used most often. To verify the pipe model, a test set up is created where the new pipe model is compared with established pipe models. As a reference, the L4 pipe model of the ClaRa library and the plug-flow pipe model of the IBPSA library are used. The Clara model has a detailed description of the physical behavior of a pipe flow and can therefore be used to check physical assumptions. For example, it is suitable for checking if the assumptions about constant fluid properties are legit. The IBPSA pipe model has been validated several times with a real DHN test setup and is known to have good accuracy [4]. It is used to determine if the pipe is representing the thermal inertia correctly.

The simulation results of these models can be seen in Fig. 7. The input for the simulation is a temperature step, which happens at 3600 s.

Table 1

Error of the output temperature of the new pipe models compared to the output temperature of the IBPSA plug-flow pipe after a temperature step.

Component	Input	Compared variable	Max. deviation	RMSE
Pipe $\Delta x = 5$ m	10 K	T_{out}	4.18 K	1.21 K
Pipe $\Delta x = 1$ m	10 K	T_{out}	3.68 K	0.66 K

Table 2

Error of the test models compared to the models of the ClaRa library.

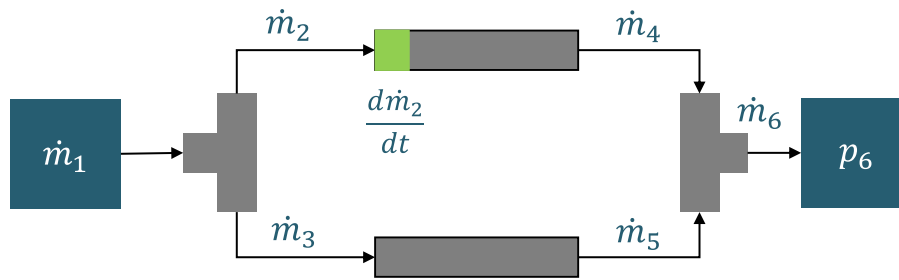
Component	Input	Compared variable	Max. deviation	RMSE
Heat exchanger	10 K step	T_{out}	0.024 K	0.012 K
Heat exchanger	10 K step	\dot{Q}	11.86 W	6.18 W
Junction	Stationary	\dot{m}	–	–
Pipe	10 K step	T_{out}	0.043 K	0.034 K

The comparison criterion is the root mean squared error (RMSE) of the outlet pipes temperature. The inlet temperature of the pipes is represented in blue. The new pipe model was simulated with a discretization length of 1 m and 5 m. For the simulation with a discretization length of 5 m the pipe has been instantiated twice. In one of the instances, the thermal capacity of the pipe wall was neglected to make it comparable to the ClaRa model. The ClaRa model was accordingly simulated with a discretization length of 5 m. The outlet temperature of the new pipe model and the ClaRa model have an accurate fit. That is why, the difference cannot be seen in the simulation.

The simulation with a discretization of 5 m has good accuracy in terms of the time constant and also a small mean error. It can be seen that the pipe wall capacity is necessary to regard because the turning point of the ClaRa pipe temperature does not fit the turning point of the IBPSA pipe. This was also determined in [41]. The results of the verification for the pipe with the IBPSA model can be seen in Table 1. The other component models like junctions and heat exchangers used in this publication have been verified with the ClaRa library as well. The results of this verification can be seen in Table 2. It can be concluded that the accuracy of the used models is sufficient.

5. Case study

In this section, a simulation of a large-scale DHN is performed. The simulation of DHNs is necessary for energetic assessments, for example, the determination of the heat losses or the electric energy needed for



Screenshot of the statistics in Dymola:

Sizes of linear systems of equations: { }
 Sizes after manipulation of the linear systems: { }
 Sizes of nonlinear systems of equations: { }
 Sizes after manipulation of the nonlinear systems: { }
 Number of numerical Jacobians: 0

Fig. 5. An example of a hydraulic circuit with a mass flow state.

System of equations

Order of computation:

- First
- Second
- Last

- I. $\dot{m}_1 + \dot{m}_2 + \dot{m}_3 = 0$
- II. $p_1 - p_2 = \dot{m}_2 \cdot \frac{\Delta p_{nom}}{\dot{m}_{nom}}$
- III. $p_1 - p_3 = \dot{m}_3 \cdot \frac{\Delta p_{nom}}{\dot{m}_{nom}}$
- IV. $\dot{m}_2 + \dot{m}_4 = 0$
- V. $p_2 - p_4 = \frac{d\dot{m}_2}{dt} \cdot L + \dot{m}_2^2 \cdot \frac{\Delta p_{nom}}{\dot{m}_{nom}^2}$
- VI. $\dot{m}_3 + \dot{m}_5 = 0$
- VII. $p_3 - p_5 = \dot{m}_3^2 \cdot \frac{\Delta p_{nom}}{\dot{m}_{nom}^2}$
- VIII. $\dot{m}_4 + \dot{m}_5 + \dot{m}_6 = 0$
- IX. $p_4 - p_6 = \dot{m}_4 \cdot \frac{\Delta p_{nom}}{\dot{m}_{nom}}$
- X. $p_5 - p_6 = \dot{m}_5 \cdot \frac{\Delta p_{nom}}{\dot{m}_{nom}}$

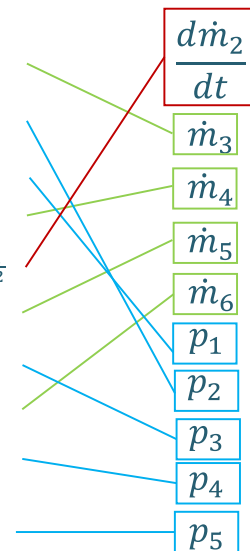


Fig. 6. Structural graph of the hydraulic circuit.

the circulation pumps. Moreover, since the thermal inertia of the piping network is considered, it is possible to investigate the shifting of the heat production by raising or lowering the supply temperature. This can be especially useful in the context of sector coupling when DHNs are used for congestion management of the electricity sector. The question arises for how long an electrical consumer, like a large-scale heat pump, can be regulated down within the scope of its technical restrictions. The time it takes for a supply temperature change to propagate through the network is the time between two static operation points, and therefore can only be determined by a dynamic simulation.

5.1. Description of the model

To test the modeling concept with regard to performance and efficiency, a DHN with 2167 substations was created. The characteristic of the network can be seen in Table 3. To design it as realistically as possible, typical distribution topologies are combined with a typical

Table 3

Characteristics of the simulated DHN.	
Number of substations	2167
Number of meshes	11
Network length	140 km

main topology. For example, in [17], six typical housing structures were identified and used for a coupled simulation. From these housing structures, four were picked for this study to design a district heating topology.

In one of the four topologies, a mesh was included, as most large-scale DHNs contain meshes. The four distribution topologies were then combined with possible main topologies according to [45]. In this book, the main topologies are categorized into five different types of DHN based on the position of the producer. For example, a producer could be integrated directly into the network or could be on the periphery. It

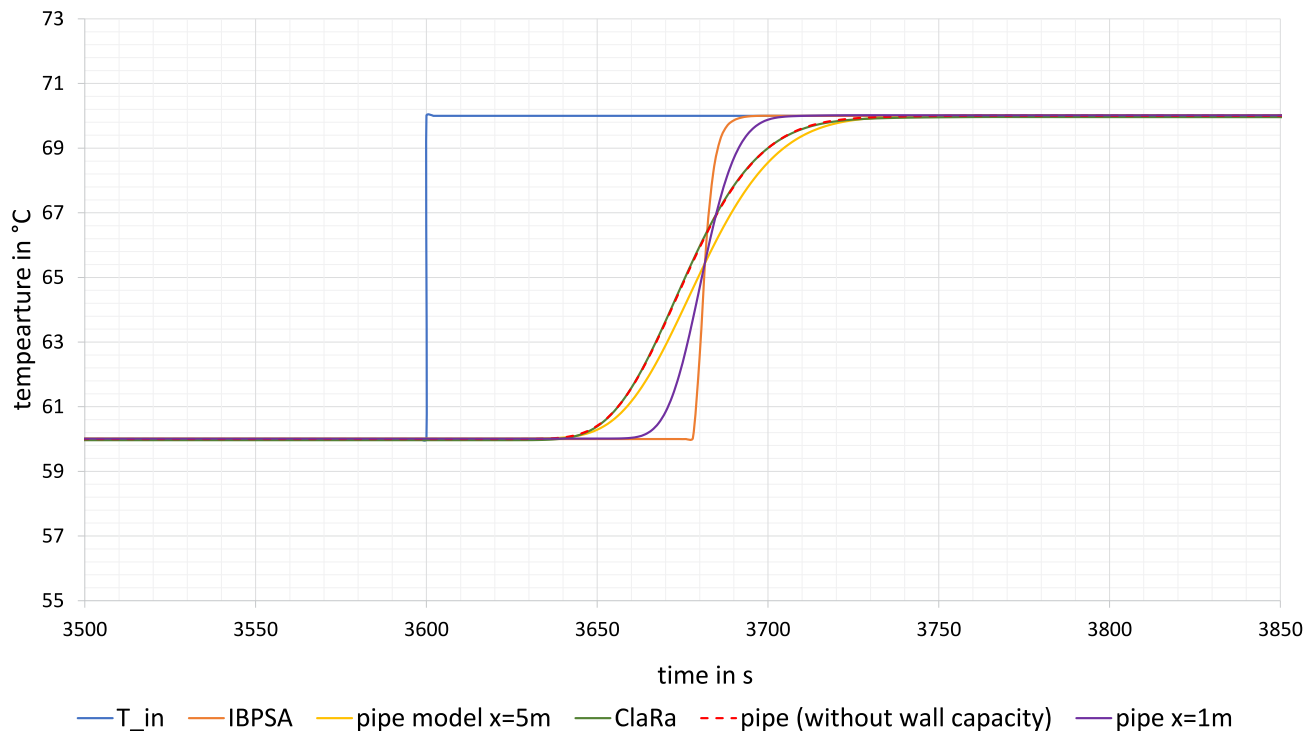


Fig. 7. Temperatures of the different pipe models for verification.

also differs between peak load and base load heat producers. For this paper, a grid topology with a heat producer on the periphery is chosen. In reality, this producer position could represent networks like those in Hamburg or Prag [45]. The presentation of the network is shown in Fig. 8.

The required variables in the simulation models are calculated as follows: Mass flow rates are calculated in the consumer models. They can be used to calculate the pressure difference over the pipes. An exception occurs in the meshes. Here the mass flow rates are a solution of the hydraulic calculation and are computed according to Section 3.7. The absolute pressure at the producer outlet is dictated behind the circulation pump. The pressure difference at this pump is controlled by a PI controller. This PI controller sets the pressure difference at the consumer in such a way that a minimum pressure difference at the consumer farthest away from the producer is kept.

The model of the DHN is based on the fact that the operator has two possibilities for changing the mass flow rate in the DHN. The pressure difference provided by the pumping stations or the supply temperature could be changed. However, changing the pressure difference could lead to an undercut of the minimum pressure difference at the substations further away from the producer. The second option is to change the supply temperature, leading to a higher temperature difference in the substations and therefore reducing the needed mass flow rate. For this case study, three load conditions of the DHN have been investigated:

- 40 percent of the max. load
- 60 percent of the max. load
- 80 percent of the max. load.

Three simulations were made with a prescribed supply temperature to demonstrate how heat production can be shifted from one hour to another by using the thermal inertia of the pipe network. A change of the supply temperature of 10 K is specified in all three scenarios. For comparison purposes, three reference simulations with a constant supply temperature under the same conditions were made.

5.2. Results

The supply temperature used as an input for the simulation are shown in Fig. 9, exemplary for the 60 percent load case. The figure displays the supply temperature at the outlet of the producer, the supply temperature at the outlet of the first pipe, and the supply temperature at a consumer being far away from the producer. The change in supply temperature contains three phases. In the first phase, the supply temperature is raised by 10 K in an hour. In the second phase, the higher supply temperature is held for three hours, and after that, the supply temperature is lowered back to the initial supply temperature. It can be seen that the supply temperature at the pipe outlet is delayed due to the flow velocity of the fluid. The same effect can be observed with the supply temperature at the consumer. However, it is much more delayed and a little lower due to the heat losses occurring in the piping network. Furthermore, the temperature at the consumer is smoother than the supply temperature at the producer. The change in supply temperature is coupled with a change in the heat provision from the heat producer. In Fig. 9 oscillations of the temperatures occur. These oscillations are due to numerical effects of the discretization but are not effecting the overall results in a major way.

The change in supply temperature leads to a change of the heat flow rate of the producer if the mass flow rate stays constant. This effect can be seen in Fig. 10. Fig. 10 shows the heat flow rate provided by the producer for the three load cases and their reference simulation. The 80 percent case is represented in yellow. The 60 percent load case is in red, and the 40 percent load case is in dark blue. In every scenario, the heat flow rate increases when the supply temperature is increased. The rate of increase, increases with a higher load on the network. This is because the mass flow rate flowing through the DHN is much higher when high loads occur.

In the 40 percent load case scenario, the heat flow rate increases after the temperature rises and stays stable for a short period of time before starting to drop again. Due to the change in supply temperature, the substations start to reduce the mass flow rate when the raised

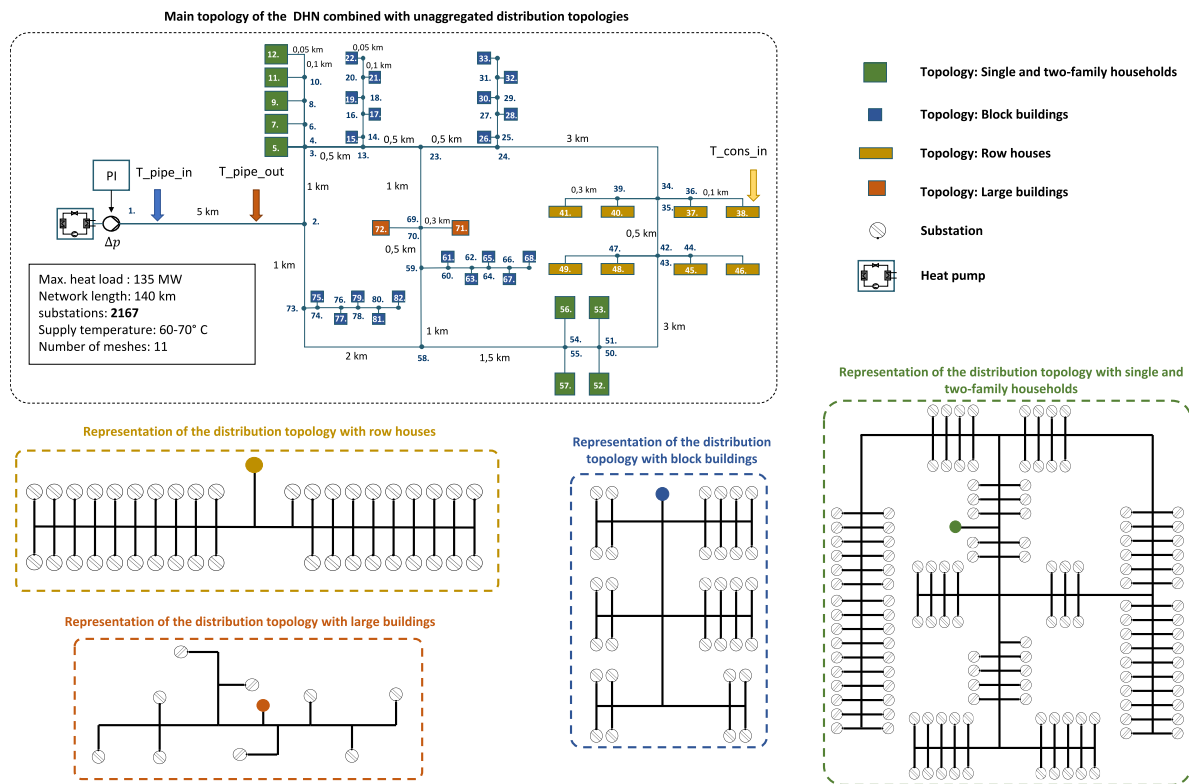


Fig. 8. Structure of the simulated DHN.

Table 4
 Time constants of the DHN at different load conditions.

Scenario	Time constant of network
40% load case	6 h
60% load case	4.25 h
80% load case	3.5 h

supply temperature arrives. Because of the thermal inertia of the DHN, this happens delayed according to the position of the substation in the network. After the supply temperature at the producer is lowered again, the heat flow rate decreases rapidly and sinks below the reference simulation. The heat flow rate stays decreased for six hours but begins to rise again after 1.5 h. In the scenarios with a higher load, there is a higher change of the heat flow rate due to the larger mass flow rate in the DHN. The higher mass flow rate also leads to a lower time constant of the system. It can be concluded that the time constant of the system and the time it takes for temperature change to propagate through the network decrease with the height of the load. The time constants for the different load cases can be seen in Table 4.

The presented model can be used to evaluate the energetic efficiency of the DHN. In Fig. 11, the heat losses, the COP of the heat pump, the pumping power, and the total consumed electric power are shown. The evaluation of efficiency is based on three effects that happen due to an increased supply temperature and a decreased mass flow rate. Due to the increased supply temperature, the COP of the heat pump decreases because the efficiency of the thermodynamic process decreases. Moreover, heat losses increase due to the higher temperature difference between the soil and the pipes. On the other hand, the pumping power needed is reduced due to the decreased mass flow rate in the network. The overall consumed electric power increases with the supply temperature but decreases when the supply temperature is

lowered again. From the diagram of the consumed electric power, it can be seen that the increase in electric power is higher than the decrease. This is because the dominant factor in the efficiency evaluation is the decrease of the COP of the heat pump rather than the saved pumping power.

To ensure that the models can be used fully open-source, a test in OpenModelica was made. For this purpose, a smaller DHN with 852 consumers was created because there were problems simulating the larger model in OpenModelica. The topology of the model can be seen in Fig. 12. The simulation is done both in OpenModelica and Dymola to compare the results in terms of accuracy and simulation efficiency. The solver Dassl [44] is used in for both simulations. In Fig. 13, the heat flow rate and the consumed electric power of the heat pump are shown for both the Dymola and the OpenModelica simulations.

It can be checked that the results are identical. However, the simulation in Dymola is substantially faster than the simulation in OpenModelica. The total simulation time consists of the translation time of the model and the pure simulation time. When simulating in Dymola, the model took two minutes for the translation and six minutes for the simulation. In contrast, OpenModelica needed one hour for the translation and 1.5 h for the simulation of the model.

6. Conclusion

In this paper, an open source modeling approach for the simulation of large-scale DHN using the modeling language Modelica is presented. A simplifying approach is used to try to avoid unnecessary equations and the occurrence of implicit non-linear systems. It can be used fully open source, which is proven by a simulation in the software environ-

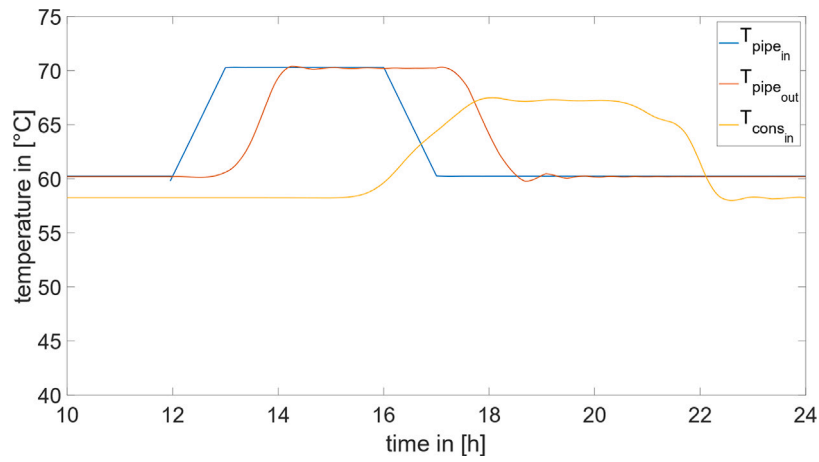


Fig. 9. Different supply temperatures in the DHN for the 60% scenario.

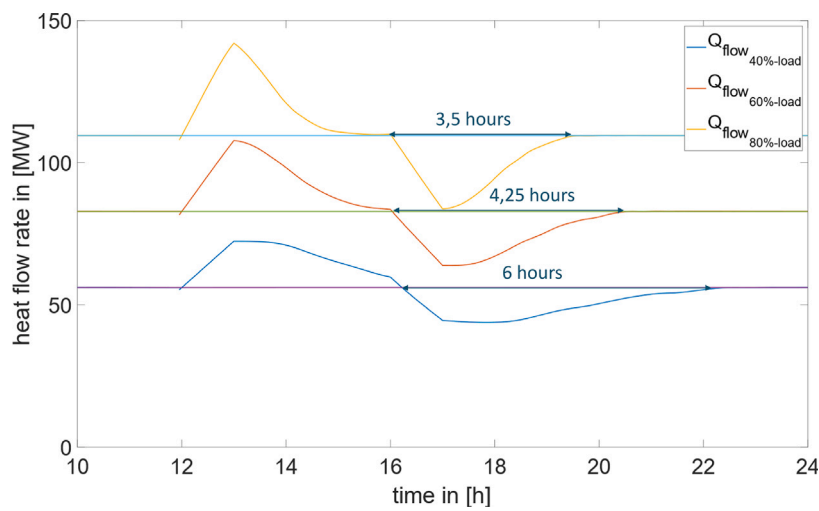


Fig. 10. Heat flow rates of the heat pump for the three scenarios.

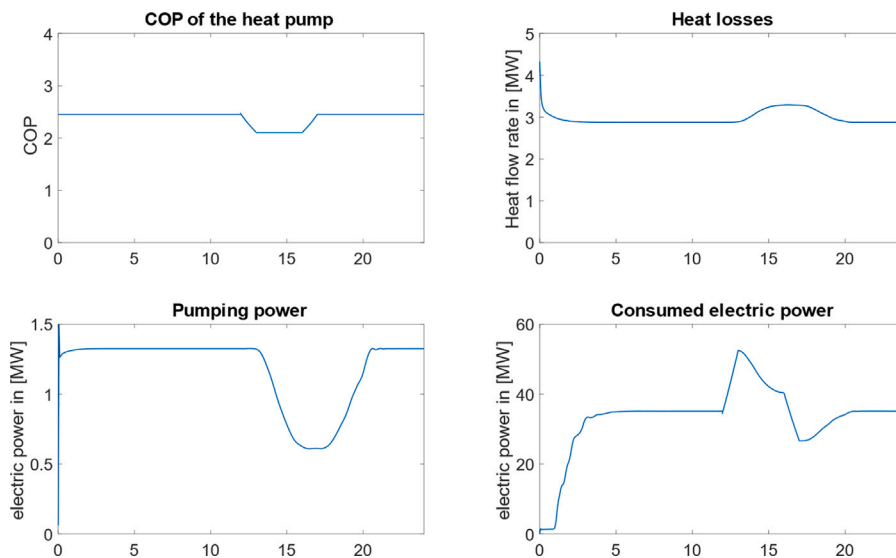


Fig. 11. Variables for the energetic assessment of the DHN for the 60% load case.

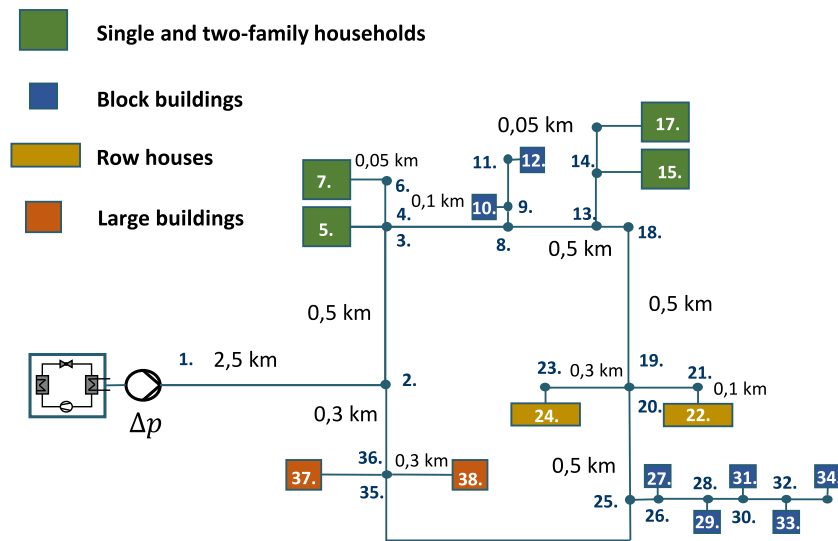


Fig. 12. Structure of the smaller DHN for the simulation in Open Modelica.

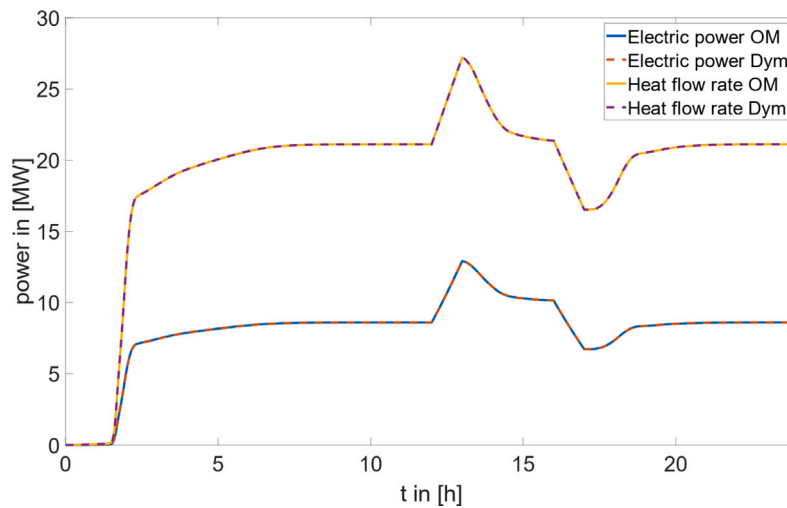


Fig. 13. Heat flow rate and electric power of the heat pump.

ment OpenModelica. The pipe models have been compared and verified with other established pipe models and can be regarded as sufficiently accurate. To prove the efficiency of the modeling concept, a DHN with over 2000 consumer models is simulated. Because the simulations took about half an hour for each, they can be considered efficient. The simulation of an exemplary DHN has shown that the time constant of the DHN changes with the mass flow rate and therefore also with the current load. A change in supply temperature changes the mass flow in the network. For this reason, the propagation of the temperature step changes over time when the increased supply temperature decreases the mass flow rate. At last, a comparison between the two software environments, Open Modelica and Dymola, was done, which showed that both can be used to simulate larger-scale DHN, although Dymola is much faster at translating and simulating the DHN model.

In future work, this modeling concept can be used for the dynamic optimization of existing large-scale DHN. In particular, this applies to the operational optimization of the DHN and central as well as decentralized heat storages. Therefore, adaptations such as taking hot water demand into account and testing the modeling concept for even larger topologies are possible next steps.

P	Power
T	Temperature
ΔT	Temperature difference
η	Efficiency factor
l	Length
L	Inertance of the pipe
d	Diameter
U	Thermal transmittance
λ	Pipe friction factor
ρ	Density of water
\dot{m}	Mass flow rate
\dot{Q}	Heat flow rate
p	Pressure
V	Volume
u	Inner energy
A	Area
s	Coordinate in flow direction
Δx	Discretization length
Subscripts	
return	Return line of DHN
supply	Supply of heat pump

source	Heat source of the heat pump
in	Ingoing flow
out	Outgoing flow
room	Room temperature in the consumer
el	Electric
hex	Heat exchanger
f	Fluid
w	Wall of the pipe
ground	Ground around the buried pipe
ext	External
Abbreviations	
DHN	District heating network
COP	Coefficient of performance of heat pump
CFD	Computational fluid dynamics

CRedit authorship contribution statement

Jan Westphal: Writing – review & editing, Writing – original draft, Visualization, Validation, Software, Resources, Methodology, Investigation, Formal analysis, Data curation, Conceptualization. **Johannes Brunnemann:** Writing – review & editing, Methodology. **Arne Speerforck:** Writing – review & editing, Supervision, Project administration, Methodology, Funding acquisition, Conceptualization.

Declaration of competing interest

The authors declare that they have no known competing financial interests or personal relationships that could have appeared to influence the work reported in this paper.

Acknowledgments

This project is funded by the German Federal Ministry of Economics and Climate Protection (BMWK) as part of the joint project “EffizientEE - Efficient integration of high shares of renewable energies in technically and economically integrated energy systems” (funding code: 03EI1050A).

Data availability

Data will be made available on request.

References

- [1] Lund H, Werner S, Wiltshire R, Svendsen S, Thorsen JE, Hvelplund F, Vad Mathiesen B. 4th generation district heating (4GDH): Integrating smart thermal grids into future sustainable energy systems. *Energy* 2014;68:1–11. <http://dx.doi.org/10.1016/j.energy.2014.02.089>, URL <https://www.sciencedirect.com/science/article/pii/S0360544214002369>.
- [2] Connolly D, Lund H, Mathiesen B, Werner S, Möller B, Persson U, Boermans T, Trier D, Østergaard P, Nielsen S. Heat roadmap europe: Combining district heating with heat savings to decarbonise the EU energy system. *Energy Policy* 2014;65:475–89. <http://dx.doi.org/10.1016/j.enpol.2013.10.035>, URL <https://www.sciencedirect.com/science/article/pii/S0301421513010574>.
- [3] Hennessy J, Li H, Wallin F, Thorin E. Flexibility in thermal grids: a review of short-term storage in district heating distribution networks. *Energy Procedia* 2019;158:2430–4. <http://dx.doi.org/10.1016/j.egypro.2019.01.302>, URL <https://www.sciencedirect.com/science/article/pii/S1876610219303224>.
- [4] Schweiger G, Heimrath R, Falay B, O'Donovan K, Nageler P, Pertschy R, Engel G, Streicher W, Leusbrock I. District energy systems: Modelling paradigms and general-purpose tools. *Energy* 2018;164:1326–40. <http://dx.doi.org/10.1016/j.energy.2018.08.193>, URL <https://www.sciencedirect.com/science/article/pii/S0360544218317274>.
- [5] Schweiger G, Larsson P-O, Magnusson F, Lauenburg P, Velut S. District heating and cooling systems – Framework for modelica-based simulation and dynamic optimization. *Energy* 2017;137:566–78. <http://dx.doi.org/10.1016/j.energy.2017.05.115>, URL <https://www.sciencedirect.com/science/article/pii/S0360544217308691>.
- [6] Kunturova S, Lickleder T, Huynh T, Zinsmeister D, Hamacher T, Perić V. Design and simulation of district heating networks: A review of modeling approaches and tools. *Energy* 2024;305:132189. <http://dx.doi.org/10.1016/j.energy.2024.132189>, URL <https://www.sciencedirect.com/science/article/pii/S0360544224019637>.
- [7] Modelica Association. Modelica. 2024, URL <https://specification.modelica.org/>.
- [8] Dassault Systèmes. Dymola 2024. 2024, URL <https://www.3ds.com/products/catia/dymola>.
- [9] Boghetti R, Kämpf JH. Verification of an open-source python library for the simulation of district heating networks with complex topologies. *Energy* 2024;290:130169. <http://dx.doi.org/10.1016/j.energy.2023.130169>, URL <https://www.sciencedirect.com/science/article/pii/S0360544223035636>.
- [10] Hirsch H, Nicolai A. An efficient numerical solution method for detailed modelling of large 5th generation district heating and cooling networks. *Energy* 2022;255:124485. <http://dx.doi.org/10.1016/j.energy.2022.124485>, URL <https://www.sciencedirect.com/science/article/pii/S0360544222013883>.
- [11] OpenModelica. OpenModelica. 2024, URL <https://openmodelica.org/>.
- [12] Dancker J, Wolter M. Improved quasi-steady-state power flow calculation for district heating systems: A coupled Newton-Raphson approach. *Appl Energy* 2021;295:116930. <http://dx.doi.org/10.1016/j.apenergy.2021.116930>, URL <https://www.sciencedirect.com/science/article/pii/S0306261921004104>.
- [13] ClaRa Development Team. Clara. 2023, URL <https://github.com/xrg-simulation/ClaRa-official>.
- [14] Senkel A, Bode C, Heckel J-P, Schülting O, Schmitz G, Becker C, Kather A. Status of the transient library: Transient simulation of complex integrated energy systems. In: *Modelica conferences*. 2021, p. 187–96.
- [15] International Building Performance Simulation Association. IBPSA. 2018, URL <https://github.com/ibpsa/modelica-ibpsa>.
- [16] TLK Thermo GmbH. TIL media. 2023, URL <https://www.tlk-thermo.com/index.php/en/software/38-til-suite>.
- [17] Benthin J, Hagemeyer A, Heyer A, Huismann P, Krassowski J, Settgaat C, et al. *Integranet abschlussbericht*. 2020, URL https://integranet.energy/wp-content/uploads/2020/04/IntegraNet-Abschlussbericht_V1.1.pdf.
- [18] van der Heijde B, Fuchs M, Tugores CR, Schweiger G, Sartor K, Basciotti D, Müller D, Nytsch-Geusen C, Wetter M, Helsen L. Dynamic equation-based thermo-hydraulic pipe model for district heating and cooling systems. *Energy Convers Manage* 2017;151:158–69. <http://dx.doi.org/10.1016/j.enconman.2017.08.072>, URL <https://www.sciencedirect.com/science/article/pii/S0196890417307975>.
- [19] Meibodi SS, Rees S, Loveridge F. Modeling district heating pipelines using a hybrid dynamic thermal network approach. *Energy* 2024;290:130107. <http://dx.doi.org/10.1016/j.energy.2023.130107>, URL <https://www.sciencedirect.com/science/article/pii/S0360544223035016>.
- [20] Dénarié A, Aprile M, Motta M. Dynamical modelling and experimental validation of a fast and accurate district heating thermo-hydraulic modular simulation tool. *Energy* 2023;282:128397. <http://dx.doi.org/10.1016/j.energy.2023.128397>, URL <https://www.sciencedirect.com/science/article/pii/S0360544223017917>.
- [21] AIT-IES. DisHeatLib. 2022, URL <https://github.com/AIT-IES/DisHeatLib>.
- [22] Zimmer D. Robust object-oriented formulation of directed thermofluid stream networks. *Math Comput Model Dyn Syst* 2020;26(3):204–33. <http://dx.doi.org/10.1080/13873954.2020.1757726>.
- [23] Lohmeier D, Cronbach D, Drauz SR, Braun M, Kneiske TM. Pandapipes: An open-source piping grid calculation package for multi-energy grid simulations. *Sustainability* 2020;12(23). <http://dx.doi.org/10.3390/su12239899>, URL <https://www.mdpi.com/2071-1050/12/23/9899>.
- [24] Ingenieurbüro Fisher-Uhrig. STANET. URL <https://www.stafu.de/de/home.html>.
- [25] Hussein A, Klein A. Modelling and validation of district heating networks using an urban simulation platform. *Appl Therm Eng* 2021;187:116529. <http://dx.doi.org/10.1016/j.applthermaleng.2020.116529>, URL <https://www.sciencedirect.com/science/article/pii/S1359431120340035>.
- [26] Steinegger J, Wallner S, Greiml M, Kienberger T. A new quasi-dynamic load flow calculation for district heating networks. *Energy* 2023;266:126410. <http://dx.doi.org/10.1016/j.energy.2022.126410>, URL <https://www.sciencedirect.com/science/article/pii/S0360544222032960>.
- [27] Falay B, Schweiger G, O'Donovan K, Leusbrock I. Enabling large-scale dynamic simulations and reducing model complexity of district heating and cooling systems by aggregation. *Energy* 2020;209:118410. <http://dx.doi.org/10.1016/j.energy.2020.118410>, URL <https://www.sciencedirect.com/science/article/pii/S0360544220315176>.
- [28] Bavière R, Vallée M. Optimal temperature control of large scale district heating networks. *Energy Procedia* 2018;149:69–78. <http://dx.doi.org/10.1016/j.egypro.2018.08.170>, URL <https://www.sciencedirect.com/science/article/pii/S1876610218304661>.
- [29] Larsen HV, Bøhm B, Wigbels M. A comparison of aggregated models for simulation and operational optimisation of district heating networks. *Energy Convers Manage* 2004;45(7):1119–39. <http://dx.doi.org/10.1016/j.enconman.2003.08.006>, URL <https://www.sciencedirect.com/science/article/pii/S0196890403002140>.
- [30] Capone M, Guelpa E, Verda V. Optimal installation of heat pumps in large district heating networks. *Energies* 2023;16(3). <http://dx.doi.org/10.3390/en16031448>, URL <https://www.mdpi.com/1996-1073/16/3/1448>.

- [31] Fuchs M, Muller D. Automated design and model generation for a district heating network from OpenStreetMap data. In: Proceedings of the 15th IBPSA conference, san francisco, CA, USA. 2017, p. 7–9.
- [32] Guelpa E, Verda V. Compact physical model for simulation of thermal networks. *Energy* 2019;175:998–1008. <http://dx.doi.org/10.1016/j.energy.2019.03.064>, URL <https://www.sciencedirect.com/science/article/pii/S0360544219304682>.
- [33] Hägg R. Dynamic simulation of district heating networks in dymola (Ph.D. thesis), Lund: Lund University; 2016, URL <https://lup.lub.lu.se/luur/download?func=downloadFile&recordId=8883842&fileId=8883845>.
- [34] Wang L, Zhang S, Fu Y, Liu M, Liu J, Yan J. Usable thermal energy stored in the district heating system for peak shaving: A dynamic simulation study. *Appl Therm Eng* 2024;239:122169. <http://dx.doi.org/10.1016/j.applthermaleng.2023.122169>, URL <https://www.sciencedirect.com/science/article/pii/S1359431123021981>.
- [35] Zheng X, Sun Q, Wang Y, Zheng L, Gao X, You S, Zhang H, Shi K. Thermo-hydraulic coupled simulation and analysis of a real large-scale complex district heating network in Tianjin. *Energy* 2021;236:121389. <http://dx.doi.org/10.1016/j.energy.2021.121389>, URL <https://www.sciencedirect.com/science/article/pii/S0360544221016376>.
- [36] Blommaert M, Wack Y, Baelmans M. An adjoint optimization approach for the topological design of large-scale district heating networks based on nonlinear models. *Appl Energy* 2020;280:116025. <http://dx.doi.org/10.1016/j.apenergy.2020.116025>, URL <https://www.sciencedirect.com/science/article/pii/S0306261920314653>.
- [37] Wittenburg R, Gierow C, Pötke R, Müller K, Holtz D. Transition of district heating from fossil to renewable energies – pathways analysed by dynamic simulation. *Renew Energy Focus* 2023;45:271–86. <http://dx.doi.org/10.1016/j.ref.2023.04.008>, URL <https://www.sciencedirect.com/science/article/pii/S1755008423000364>.
- [38] Vojacek A, Brunnemann J, Hanke T, Marx-Schubach T, Eiden J. Status of the clara library: Detailed transient simulation of complex energy systems. In: Modelica conferences. 2023, p. 617–26, URL <https://doi.org/10.3384/ecp204617>.
- [39] Franke R, Casella F, Otter M, Sielemann M, Elmqvist H, Mattson SE, Olsson H. Stream connectors - an extension of modelica for device-oriented modeling of convective transport phenomena. In: Casella (hg.) 2009 – proceedings of the 7th international modelica conference. p. 108–21, URL <https://elib.dlr.de/62362/>.
- [40] Vahlenkamp T, Wischhusen S. FluidDissipation-A centralised library for modelling of heat transfer and pressure loss. In: Proceedings of the 6th international modelica conference. Vol. 1, p. 173–8, URL <https://citeseerx.ist.psu.edu/document?repid=rep1&type=pdf&doi=ea018ed5b68179fa9a8ad00a8ae63fed21b3df44>.
- [41] Capone M, Guelpa E, Verda V. Accounting for pipeline thermal capacity in district heating simulations. *Energy* 2021;219:119663. <http://dx.doi.org/10.1016/j.energy.2020.119663>, URL <https://www.sciencedirect.com/science/article/pii/S0360544220327705>.
- [42] Speerforck A, Ling J, Aute V, Radermacher R, Schmitz G. Modeling and simulation of a desiccant assisted solar and geothermal air conditioning system. *Energy* 2017;141:2321–36. <http://dx.doi.org/10.1016/j.energy.2017.11.151>, URL <https://www.sciencedirect.com/science/article/pii/S0360544217320091>.
- [43] Senkel A. Vergleich verschiedener Arten der Wärmeverbrauchermodellierung in Modelica (Ph.D. thesis), Hamburg: Hamburg University of Technology; 2017.
- [44] Petzold LR. Description of DASSEL: a differential/algebraic system solver. 1982, URL https://www.osti.gov/biblio/5882821_journal.
- [45] Frederiksen S, Werner S. District heating and cooling. first ed.. Lund: Studentlitteratur AB; 2013.